Journal of the Iranian Chemical Society (2019) 16:2555–2564
https://doi.org/10.1007/s13738-019-01718-y

ORIGINAL PAPER

A signal amplification by QDs used for ferrocene-labeled sandwich aptasensor for determination of Hg^{2+} in water samples

Hosna Ehzari[1] · Meysam Safari[2] · Mohsen Shahlaei[3]

Received: 4 November 2018 / Accepted: 17 June 2019 / Published online: 19 July 2019

Abstract

In this paper, the design of a novel sandwich-type electrochemical aptasensor was reported for an ultrasensitive mercury ion (Hg^{2+}) detection in water samples, which labeled with two-labeled aptamer (Apt) sequences. The used Apts were Apt1 and Apt2 as the capture and signal probe, respectively. The Apt1 probe was immobilized on the poly(4-aminobenzoic acid) (p-ABA) and quantum dots (QDs) film as the platform, as well as the Apt2 reporter was labeled with ferrocene. In the presence of Hg^{2+}, the strong coordination complex has been formed between the specific thymine of the Apt1, Hg^{2+}, as well as the thymine of the Apt as T–Hg^{2+}–T adduct. The QDs and p-ABA were applied for increasing the conductivity of platform and suitable binding of the recognition elements. Under the optimized conditions, the constructed aptasensor illustrated either a wide linear relationship between the logarithm of Hg^{2+} concentration and current, from 0.05 to 100 nM and also an excellent low limit of detection of 0.01 nM. The quality of carefully choosing, an excellent stability and specificity sensitivity of the designed aptasensor, was investigated by spiked tap water samples as real sample. Moreover, the aptasensor exhibits the good reproducibility as well as has high selectivity for the other cations. The recoveries of the Hg^{2+} assay of the tap water samples were acquired satisfactorily which imply the generated aptasensor can use Hg^{2+} measurement in the real laboratories.

Keywords Mercury ion · Electrochemical aptasensor · Poly(4-aminobenzoic acid) · Quantum dots · Glassy carbon electrode

Introduction

One of the most well-known toxic heavy metal ions is the mercury ion. Hg^{2+} is the most stable inorganic form of mercury that is commonly produced by industrial manufactories effluent. According to the scientific findings, accumulation of Hg^{2+} in the human body through the daily food and drink can cause serious damages to the vital organs such as intestines and kidney. Also, accumulation of Hg^{2+} in the human body can make erythrism as well as arrhythmia, central nervous system defects and damage to the stomach [1, 2]. According to United States Environmental Protection Agency (EPA) guidelines, the maximum acceptable concentration (MAC) for Hg^{2+} in drinking water is 10 nM [3]. Therefore, development of a sensitive and rapid procedure for Hg^{2+} determination is essential.

Heretofore, various analytical techniques have been applied to Hg^{2+} detection and analysis, such as atomic emission spectrometry [4], and fluorescence [2, 5–7], colorimetric analysis [8], luminescence [9], mass spectrometry [10], atomic absorption spectrometry [11], UV–Vis [12] and inductively coupled plasma mass spectrometry (ICP-MS) [13]. While almost all these analytical methods are sensitive, selective and accurate, there are some limitations and disadvantages, such as expensive instrumentation, requiring to pretreatment steps, time-consuming sample preparation steps and large amounts of samples. Electrochemical procedures have all the merits and represent low-cost alternatives.

Electronic supplementary material The online version of this article (https://doi.org/10.1007/s13738-019-01718-y) contains supplementary material, which is available to authorized users.

✉ Mohsen Shahlaei
mohsenshahlaei@yahoo.com

[1] Nano Drug Delivery Research Center, Health Technology Institute, Kermanshah University of Medical Sciences, Kermanshah, Iran

[2] Department of Chemical Engineering, Kermanshah University of Technology, Kermanshah, Iran

[3] Medical Biology Research Center, Health Technology Institute, Kermanshah University of Medical Sciences, Kermanshah, Iran

These methods have a considerable reproducibility and a rapid response time. As well as often associated low LOD, along with the simplicity of preparation of the electrochemical sensors, have been generated extensive interest. Therefore, the choice of a substitute procedure accompanied by lower operating cost and effective detection speed for assessment of the low level of Hg^{2+} is a challenging endeavor. A number of studies based on electrochemical methods have been reported to date for Hg^{2+} detection [14–18]. In recent years, the sandwich-format aptasensors compared to other aptasensor have acquired lots of attention due to their superior features, such as the shorter measurement time, the lower limit of detection, higher selectivity in the presence of many interferes and miniaturizable instrumentation [19–21]. To assess the ultra-low amount of Hg^{2+} in samples, various types of signal amplification strategies have been reported specially by the labeled Apts [22–25]. Some labels have been explored as signaling species including ferrocene, metal nanoparticles [26, 27] and methylene blue [28, 29]. Ferrocene has been widely employed as a label for electrochemical detection of ions [7, 30–32].

The modified electrodes have advantages such as low background currents, wide potential range, low cost, easy construction and fast surface reducibility. In these electrodes, various modifiers can be utilized to catalyze the oxidation–reduction processes and facilitate the electron transfer. Nanostructures owing to their supernatural physicochemical attributes have been gained in the area of biosensing, recently.

Quantum dots (QDs), due to the quantum confinement effect and the extent of their energy band gap, have useful optical and electrical properties [33–35]. These nanomaterials are employed widely as the signal element or amplifier in electrochemical sensors [34, 36–38]. Polymeric films have three-dimensional extensity, a large number of reactive sites, good stability and offer the possibility to be designed with particular redox active sites [39–41]. Based on the previous reports, the properties of composition polymers with inorganic nanoparticles or QDs improved the operation of the chemical analysis and sensors [42–47].

Herein, the main goal is to provide a new and sensitive sandwich-type electrochemical aptasensor which was fabricated for the sensitive detection based on the p-ABA-QDs film on the GCE surface in order that an impressive immobilization of Apts and the strong and specific binding of Hg^{2+} with two thymine (T) bases of Apts. The QDs and p-ABA were applied for increasing the conductivity of platform and suitable binding of the recognition elements. Taking advantages of QDs and p-ABA film and signal amplification, the offered aptasensor depicted a low detection limit and wide linear range. The electrochemical signal of the ferrocene-labeled Apt 2 was traced for the Hg^{2+} measurement. Moreover, this electrochemical aptasensor was evaluated in Hg^{2+} spiked tap water samples, and acceptable analytical performance was obtained.

Experimental

Reagents and chemicals

N-(3-dimethylaminopropyl)-*N*′-ethylcarbodiimide hydrochloride (EDC.HCl), p-aminobenzoic acid (p-ABA), mercaptohexanol and N-hydroxysuccinimide (NHS, 98%) were purchased from Sigma-Aldrich Co. (St. Louis, MO, USA). Potassium ferrocyanide ($K_4Fe(CN)_6$) and potassium ferricyanide ($K_3Fe(CN)_6$ were acquired from Merck Co. (Darmstadt, Germany). In these experiments, phosphate buffer saline (PBS, pH 7.4) was prepared by NaCl (100 mM), KCl (2.0 mM), Na_2HPO_4 (6.4 mM) and KH_2PO_4 (1.0 mM) and used as an incubation buffer. All experiments were accomplished at ambient temperature. An additional chemical and reagents consumed in this work were acquired as analytical grade and applied without additional purification.

The Apts of [5′-(NH_2)-TTT TTT TTT TAC AGC AGA TCA GTC TAT CTT CTC CTG ATG GGT TCC TAT TTA TAG GTG AAG CTG T-3′ and 3′-TCTCTTGTCTTCGTCT-5′- Ferrocene as probe and reporter, respectively, were synthesized and purified by Fazabiotech Co. (Tehran, Iran).

Apparatus and measurements

The electrochemical impedance spectroscopy (EIS) with a FRA 32 impedance analysis module, as well as the differential pulse voltammetry (DPV) and cyclic voltammetry (CV) experiments, were performed by an Autolab system potentiostat–galvanostat model PGSTAT 204 (Utrecht, The Netherlands) using a NOVA (1.11) software. A modified and/or bare glassy carbon electrode (GCE), platinum wire and a silver–silver chloride (Ag/AgCl, 3.0 M KCl) electrode were utilized as working, auxiliary and reference electrodes, respectively. Electrochemical impedance spectroscopy (EIS) measurements were carried out in a solution containing 0.5 mM concentration of the both $K_3Fe(CN)_6$ and $K_4Fe(CN)_6$ (1:1,) as the redox couple, under open-circuit potential (OCP) conditions with a 5 mV AC amplitude and in the frequency range of 10 kHz to 0.01 Hz.

Synthesis of QDs

To the synthesis of QDs, the previous method by M. Safari et al. has been applied [48]. Firstly, in order to prepare the sodium hydrogen telluride (NaHTe), the tellurium (Te) powder was reduced with sodium borohydride ($NaBH_4$) in deionized water under N_2 purging, while the solution was stirred strongly. After 3 h, resulting NaHTe was used in

the preparation of CdTe particles. In another flask, 0.3 g of $CdCl_2{\cdot}H_2O$ was dissolved in 40 mL of ultrapure water followed by the addition of 200 µl of TGA under stirring conditions. The pH of the reaction was adjusted up to 10 by drop-wise addition of NaOH solution (1 M). In the next step, the freshly prepared NaHTe was added to a $CdCl_2$ solution containing (TGA) under N_2 atmosphere. Then, the acquired solution after mixing was transferred into a Teflon-lined stainless steel autoclave and heated in an oven at 120 °C for 3 h. After that, the autoclave was cooled and so, thiol-capped CdTe QDs was obtained.

Fabrication of the electrochemical aptasensor

Before modification, the bare GCE was polished to a mirror-like with 0.1, 0.3 and 0.05 µm alumina slurry, and then washed successively with water–ethanol solution (1:1) in an ultrasonic bath. For making the mentioned aptasensor, at first, the cleaned GCE surface was immersed in solution containing 1 mM p-ABA and PBS as supporting electrolyte, and the p-ABA was electrochemically deposited on the GCE by CV for several cycles. Electropolymerization was achieved by cyclic sweeping between − 0.8 and 1.0 V, with a scan rate of 100 mV s^{-1}, for 15 cycles to prepare GCE/p-ABA. After the polymerization process, the electrode was washed with deionized water and subsequently, 2 µL of QDs suspension was dropped onto the surface of the p-ABA/GCE and was dried at room temperature and the constructed electrode was named as the QDs/p-ABA/GCE. Then, the fabricated sensor was dried carefully and then washed with deionized water. For activation of the sensor surface functional groups, this sensor was dipped into the 0.05 M PBS of pH 7.4 containing 20 mM EDC and 40 mM NHS for 30 min and washed with PBS. Afterward, 3 µL of Apt probe (Apt 1, 8 µM) was carefully dropped onto the pretreated GCE/p-ABA-QDs surface for 20 min. Then, the developed sensor was immersed in the mercaptohexanol (6 mM) for 30 min to block the residual active sites on working electrode, and the aptasensor washed with deionized water. Next, this electrode (denoted as GCE/p-ABA-QDs/Apt1) was kept at 4 °C for the duration of a night in a condition saturated from moisture to keeping away from evaporation of solvent and eventually, the electrode was rinsed with the PBS (0.1 M, pH 7.4) to eliminate excess physically adsorbed Apt. In the next step, the GCE/p-ABA-QDs/Apt1 was immersed into the solutions with variable concentrations of Hg^{2+} in order to form T-Hg^{2+} for 30 min. Finally, the electrode at the solution of Apt reporter (Apt2) for 30 min to acquiring the T-Hg^{2+}-T. Then, the electrode was washed carefully with a PBS (0.1 M, pH 7.4) and to retain of an immobilized Apt activity was hold at 4 °C into the buffer solution. The order of procedure for aptasensor making is illustrated in Scheme 1.

Results and discussion

Investigation of CdTe

The particle size and morphology of the CdTe was studied by TEM. It is quite evident that CdTe nanoparticles are close to a spherical shape and are uniform in size with diameter about 3–5 nm (Fig. S1).

The surface morphology and electrochemical properties studies

For investigation of the surface structure and morphology of the constructed sensor, SEM images of bare and amended electrodes were used. Figure 1 represents the SEM forms of GCE (A), and GCE/p-ABA-QDs (B). As it can be seen in Fig. 1B, the p-ABA-QDs particles (B) have a spherical grains by forming nanostructure aggregations and its morphology is different from that observed for GCE (A). Energy dispersive X-ray spectroscopy (EDX) image is also shown in Fig. 1C. The EDX clearly indicates the presence of different percentages of C, O, Cd and Te at the prepared composite electrode.

These observations confirm the success attaching p-ABA-QDs film on the GCE surface, which is suitable for successful performance in the next electrochemical studies and Apts immobilization.

In order to investigate the variations occurred between the interface of surface of the electrode and the solution, the EIS is often utilized. In typical EIS experiments, $[Fe(CN)_6]^{3-/4-}$ mainly was used as a probe. In these measurements, the semicircle diameter of impedance at higher frequencies is equal to the electron transfer resistance (R_{et}), which controls the electron transfer kinetics of the redox probe on the electrode surface. A change in the value of R_{et} is related to the blocking behavior of the modification processes on the electrode surface, which is reflected in the EIS as a change in the diameter of the semicircle at high frequencies [49, 50].

Figure 2 introduces the Nyquist plots during stepwise modification of GCE in a solution containing $[Fe(CN)_6]^{3-/4-}$ (0.5 mM) and KCl (0.1 M). The Nyquist plot of the bare electrode gives a high semicircle domain (curve a). The shapes of the Nyquist plots of GC/p-ABA and GC/p-ABA-QDs electrodes are the same as that of a naked GCE, but with a lower semicircle diameter, and the R_{ct} values are about 1000 and 487 Ω, respectively. Decreasing the amounts of R_{et} at the p-ABA/GC and GC/p-ABA-QDs electrodes surface indicates that conductivity of polymer and QDs nanocomposite can increase an electron transfer and so the diffusion speed of ferricyanide toward

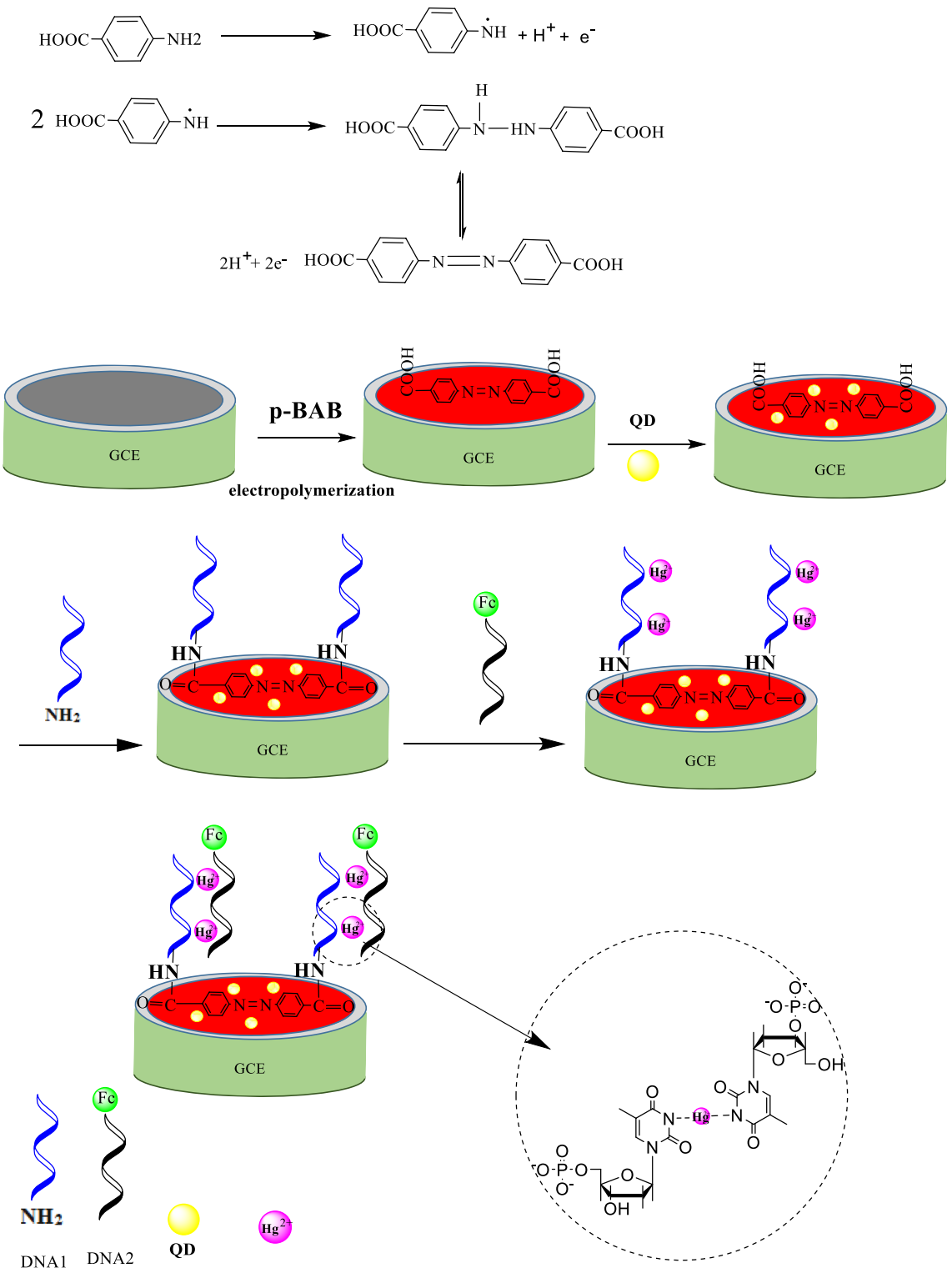

Scheme 1 Schematic illustration for fabrication of Hg^{2+} aptasensor

the electrode surface is high. Next, the EIS of GCE/p-ABA-QDs/Apt1 after successful immobilization of the Apt1 on the GCE/p-ABA-QDs was investigated (curve d). As it can be seen, after immobilization of Apt1, due to the covalent attachment of NH_2-terminated Apt sequence with the carboxylated p-ABA interface, the R_{et} value largely increased. After the GCE/p-ABA-QDs/Apt1 was placed in solution containing Hg^{2+} and then in Apt2 solution,

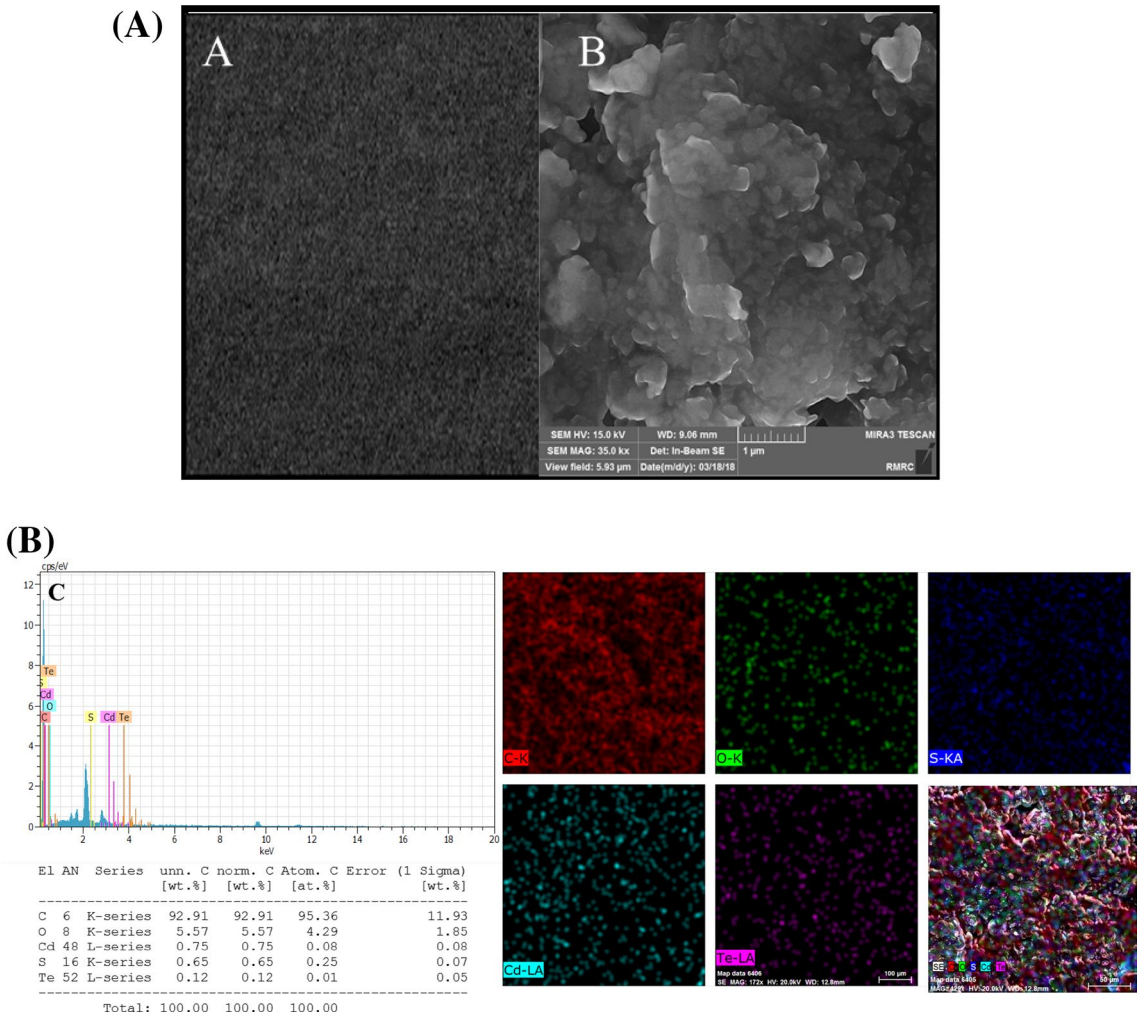

Fig. 1 SEM forms of GCE (A), GCE/p-ABA-QDs (B) and EDX spectrum and mapping recorded at GCE/p-ABA-QDs elemental different showing signal of C, O, Cd and Te, respectively, as is illustrated (C)

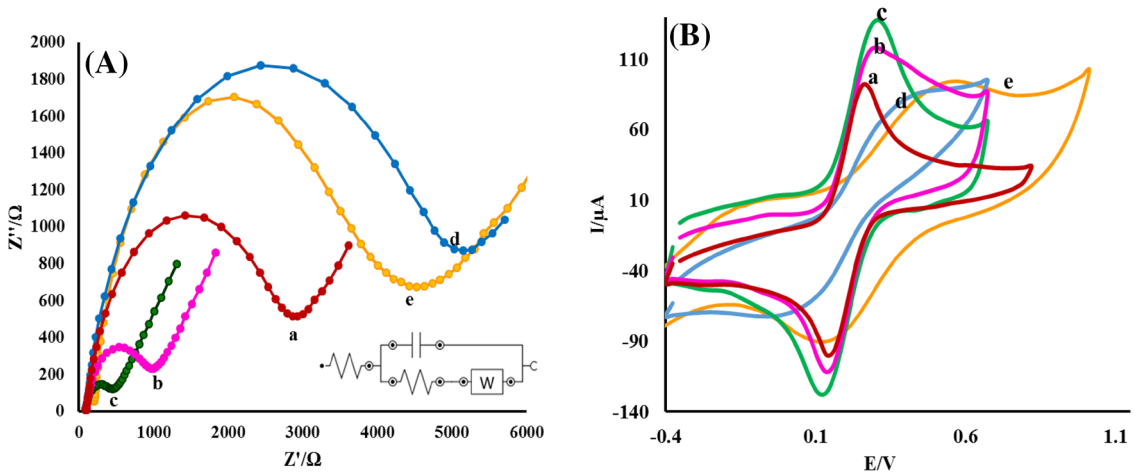

Fig. 2 Nyquist diagrams (**A**) and Cyclic voltammograms (**B**) of 0.1 M KCl solution containing 5.0 mM Fe $(CN)_6^{3/4-}$ recorded at GCE (a), GCE/p-ABA (b), GCE/p-ABA-QDs (c), GCE/p-ABA-QD/Apt1 (d) and after treatment with 10 nM of Hg^{2+} and then the Apt2 (e)

the value of R_{et} decreased slightly (curve e), which indicated the presence of Hg^{2+} in between the aptamer strings and so, its electron transfer rate and conductivity were increased at the GCE/p-ABA-QDs/Apt1 surface.

As well as, the results of the EIS were authenticated by evaluating the CVs of the above-mentioned solution containing $[Fe(CN)_6]^{3-/4-}$ (0.5 mM) and KCl (0.1 M), and these results were illustrated in Fig. 2B. After electrodeposition of p-ABA on the GCE, the redox peak currents increased (curve b) in comparison with the redox peak currents of the GCE (curve a). After deposition of QDs by dropping QDs solution on the GCE/p-ABA, the redox peak currents of electrode (curve c) were increased. As it is seen, after immobilization of Apt1 on the GCE/p-ABA-QDs surface, the peak currents significantly decreased, which confirms the successful immobilization of the Apt on GCE/p-ABA-QDs surface (curve d). When the GCE/p-ABA-QDs/Apt1 is placed into the Hg^{2+} solution and then in the Apt2 solution, the redox peak currents increases, which confirms the presence of Hg^{2+} in between the aptamer strings.

The Apt2 labeled with ferrocene was employed as the electrochemical probe for the sensitive determination of Hg^{2+} by DPV procedure. As can be seen in Fig. 3, in the absence of Hg^{2+}, the DPV peak current of ferrocene is not observed (curve a). But in the presence of the Hg^{2+}, the peak current of ferrocene appeared (curve b). The sensor response in the presence of Hg^{2+} (100 nM) without Apt 2 is relatively weak.

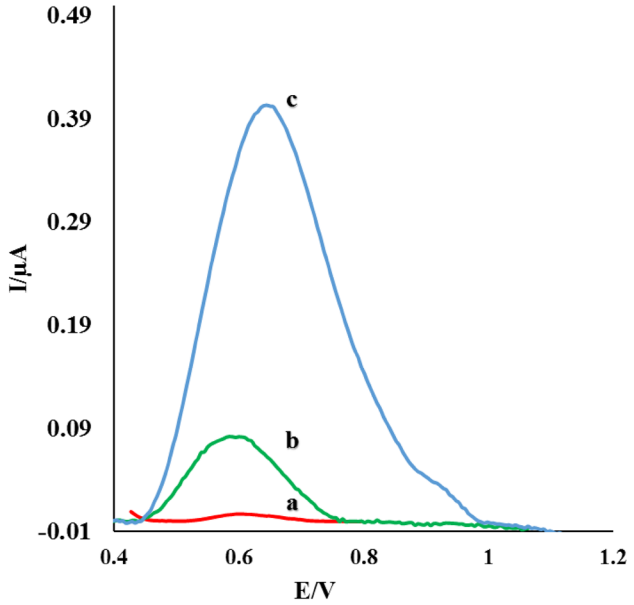

Fig. 3 DPVs of GCE/p-ABA-QDs/Apt1 (a) in the absence of Hg^{2+} and the presence of Apt2, (b) in the presence of Hg^{2+} without Apt2 and (c) in the presence of Hg^{2+} and Apt2 in a solution of PBS (0.1 M of pH 7.4)

Optimization of main experimental conditions

The important factors influencing the main experimental conditions, including the Apt probe concentration and incubation time between Hg^{2+} and Apts, were studied to enhance the sensitivity of the designed aptasensor respond which are shown in Fig. 4A. To optimize the immobilization of Apt probe, the GCE/p-ABA-QDs was dipped in the solutions containing different concentrations to immobilization of Apt probe. As can be seen in Fig. 4A, the maximum current was observed in 8 μM of Apt probe, and then with increasing the Apt concentration, the signal current of ferrocene-labeled Apt2 remained unchanged. Therefore, 8 μM was chosen as the optimal Apt concentration in the following experiments.

In the next step, the influence of the incubation time of 10 nM Hg^{2+} with the Apt1 was studied (Fig. 4B). The experimental results illustrated that the current of ferrocene was enhanced with the increase in incubation time of Hg^{2+} up to 40 min and longer incubation time did not clearly improve the response of aptasensor (Fig. 4B). So, 40 min was chosen as the optimal incubation time in the next experiments.

The incubation time of GCE/p-ABA-QDs/Apt1-Hg^{2+} with the Apt2 was also optimized for 10, 20, 30 and 40 min (Fig. 4C). The experimental results showed that the current of ferrocene was enhanced with an increase in incubation

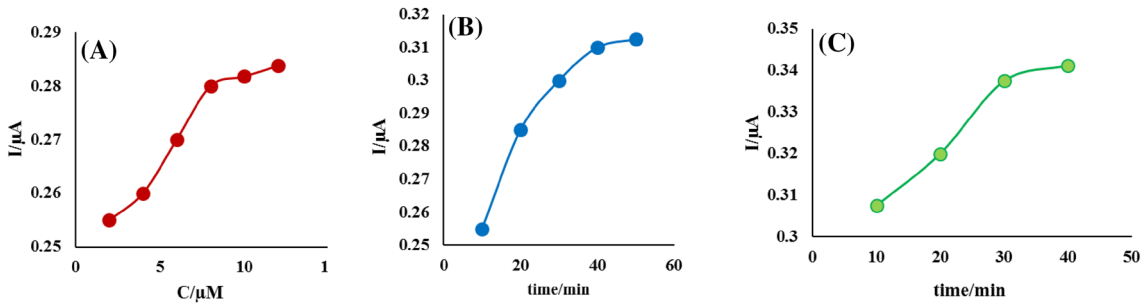

Fig. 4 DPV of GCE/p-ABA-QDs/DNA1-Hg^{2+}-Apt2 recorded in different optimization steps. **A** Immobilization of probe aptamers, **B** incubation time of 10 nM Hg^{2+} with the Apt1, **C** incubation time of Apt1- Hg^{2+} with the Apt2 in a solution of PBS (0.1 M of pH 7.4)

time of Hg^{2+} up to 30 min and longer incubation time did not obviously improve the response of designed aptasensor (Fig. 4C). So, 30 min was selected as the optimal incubation time for Apt2 interaction on the aptasensor surface.

Analytical performance of aptasensor

To assess the quantitative analysis, the sensitivity of Hg^{2+} sandwich-type aptasensor was investigated under the optimized experimental conditions in PBS (0.1 M pH 7.4). Figure 5 depicts the current responses of the GCE/p-ABA-QDs/Apt1/Apt2 as corresponded to the different concentrations Hg^{2+}.

As it is seen, the peak currents gradually increased with the enhancement in the Hg^{2+} concentration. The current was linear in proportional to the logarithm of Hg^{2+} concentration from 0.05 to 100 nM, and the regression equation was $I(\mu A) = 0.1419\ \mathrm{Log}(C_{pM}) + 0.5366$ (correlation coefficient of 0.9856.). The limit of detection (LOD) value is 0.01 nM. These results indicated that the Apts have well affinity to Hg^{2+} ion at the transducer surface. This electrochemical aptasensor was comparable to previously reported electrochemical sensors for Hg^{2+} detection, and due to the presence of p-ABA and QDs nanocomposite, illustrated a wider linear range and lower LOD. The procedure of construction of this sensor in comparison with other sensors was simple and did not need complicated interpretation, and also it was used for rapid detection of Hg^{2+} in tap water samples.

From inset of Fig. 5B, C, it can be concluded that the interaction of biochemical reaction such antibody antigens, DNA hybridization, protein–protein interaction, protein–DNA interaction and ion–DNA interactions are predominating by Michaelis–Menten relations. This mechanism explains the binding events in biochemical systems, in which the binding process become slow with increasing target concentration. In brief, the existence of such behavior can regard as the main reason that confines the magnitude of signal change obtained for a fixed time incubation [51–55]. More elucidation of such behavior aimed to be studied by our research group (Table 1).

An evaluation of the reproducibility, stability and specificity of aptasensor

The reproducibility of the GCE/p-ABA-QDs/Apt1/Apt2 was investigated under optimal conditions. The current response of six electrodes was recorded in a solution of PBS (0.1 M, pH 7.4). The relative standard deviation (RSD) of the six measurements for Hg^{2+} was acquired at 4.7% detection. The results of the RSD depicted the high reproducibility of the p-ABA-QDs/Apt1/Apt2 at the GCE surface.

The repeatability of the mentioned aptasensor was evaluated by detecting the DPV response of the six electrochemical signals of Hg^{2+} measurements (10 nM.). The RSD obtained was 3.18%, which illustrated the acceptable repeatability of this sensor.

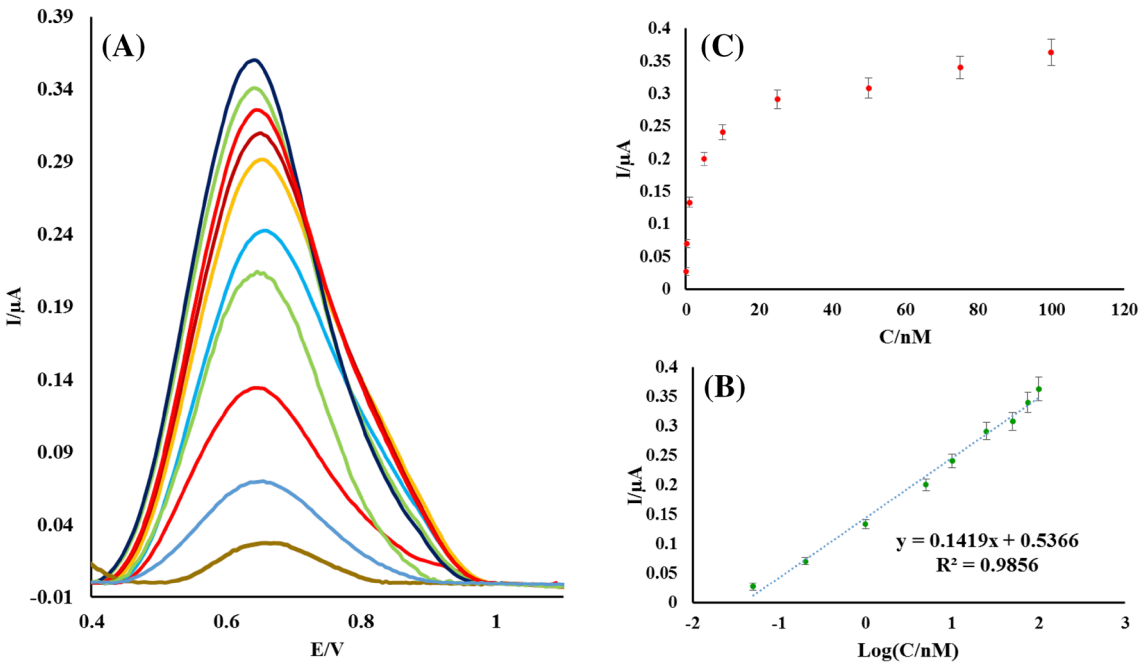

Fig. 5 **A** DPVs of GCE/p-ABA-QD/Apt1-Hg^{2+}-Apt2 recorded in different concentrations of Hg^{2+}. **B** Calibration curves of DPV peak current and **C** the linear relationship between current versus logarithmic concentration of Hg^{2+} concentration in the range 0.05–100 nM

Table 1 Comparison of analytical properties of different assays toward Hg^{2+}

Sensor fabrication	LOD	Liner range	References
Electrochemiluminescence assay	2.3 nM	5.0–500 nM	[56]
Electrochemiluminescence	0.105 nM	0.2–20 nM	[57]
Electrochemical sensor	1–300 nM	1.0 nM	[58]
Electrochemical sensor	0.03 nM	0.1–100 nM	[59]
Electrochemical sensor	0.002 nM	0.005–80 nM	[60]
Electrochemical sensor	0.02 nM	0.02–1000 nM	[61]
Impedimetric assay	0.1 nM	0.1 nM to 10 µM	[62]
Electrochemical sensor	0.06 nM	0.5 nM–120 nM	[63]
Electrochemical aptamer	0.005 pM	0.01 pM–2 pM	[64]
Electrochemical sensor	1.5 pM	0.27 pM–8.5 nM	[14]
Strip biosensor electrochemical	0.01 nM	0.01 nM-100 µM	[65]
Electrochemical/based on T–Hg^{2+}–T structure and exonuclease	6.2 pM	10 pM–100 nM	[66]
A label-free electrochemical sensor	33 pM.	100 pM–100 nM,	[67]
Electrochemilumine	5.1 pM	0.02–30 nM	[68]
Electrochemical aptasensor	0.14 pM	0.25 pM–100 nM	[69]
Electrochemical aptasensor	0.6 zM	5 zM–55 pM	[70]
Electrochemical aptasensor	0.12 nM	0.5–50 nM	[71]
Electrochemiluminescence	2 aM.	20 aM to 2 µM	[72]
Label-electrochemical sandwich aptamer	0.01 nM	0.05–100 nM	This work

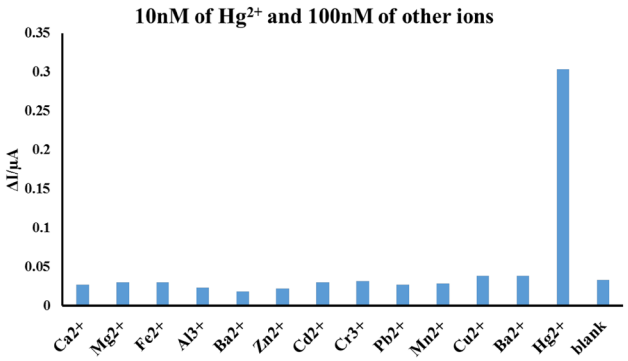

Fig. 6 Selectivity of the aptasensor. The DPV signal changes of the aptasensor to 10 nM Hg^{2+} and in the presence of various metal ions (100 nM)

For investigating the specificity of the proposed aptasensor, the response of this sensor was studied in the presence of 100 nM of some of cations such as Ca^{2+}, Mg^{2+}, Fe^{3+}, Fe^{2+}, Al^{3+}, Ba^{2+}, Zn^{2+}, Cd^{2+}, Cr^{3+}, Zn^{2+}, Pb^{2+}, Mn^{2+} and Cu^{2+}, each at a concentration of 100 nM and Hg^{2+} concentration of 10 nM and a sample without Hg^{2+} as a blank control. No significant change in DPV responses was observed except that for Hg^{2+} (Fig. 6).

The stability of the p-ABA-QD/Apt1/Apt2 was also investigated. After 18 days, the signal DPV of the aptasensor in a solution of PBS (0.1 M, pH 7.4) was recorded. So, the obtained result shows no remarkable change for the DPV peak current aptasensor after 18 days. After measuring, the constructed aptasensor was stored at 4 °C in PBS (0.1 M, pH = 7.4).

Application of aptasensor in real samples

In order to test the applicability of the offered sandwich-type aptasensor, the tap water samples were employed. The standard addition method was applied to Hg^{2+} measurement using DPV method. The results of the analysis of sandwich-type aptasensor are summarized in Table 2. As can be seen, the recoveries of the proposed aptasensor responses to Hg^{2+} measurement in tap water samples were between 104.0 and 108.5%, also the RSD of the proposed method is less than 5%, which shows the good precision of the method for Hg^{2+} monitoring using the offered method.

Table 2 Determination of Hg^{2+} in tap water samples ($n = 3$)

Sample	Added Hg^{2+}/pM	Detected Hg^{2+}/pM	Recovery (%)	R.S.D. (%)
Tap water	1000	1085.0	108.5	2.8
	3000	3090.0	103.0	2.6
	10,000	10,400.0	104.0	3.2

Conclusions

In this work, a sandwich-type aptasensing tools was fabricated for ultrasensitive detection of Hg^{2+} in water samples. The sandwich-type aptasensor was designed based on the immobilization primary aptamer (Apt1) on the poly(4-aminobenzoic acid)/quantum dots (QDs) platform, and the ferrocene (Fc)-labeled secondary aptamer (Apt2). Under the optimized conditions, the linear relationship between the logarithm of Hg^{2+} concentration and current was observed. The proposed aptasensor illustrated a linear relationship from 0.05 to 100 nM with calculated LOD of 0.01 nM. The proposed aptasensor displays reasonable stability, good reproducibility, selectivity and high sensitivity for low-level detection of Hg^{2+} sequence. As well as, the signal response of aptasensor has a satisfactory repeatability.

References

1. K.J. Powell, P.L. Brown, R.H. Byrne, T. Gajda, G. Hefter, S. Sjöberg, H. Wanner, Pure Appl. Chem. **77**, 739 (2005)
2. S. Amiri, R. Ahmadi, A. Salimi, A. Navaee, S.H. Qaddare, M.K. Amini, New J. Chem. **42**, 16027 (2018)
3. P. Miao, L. Liu, Y. Li, G. Li, Electrochem. Commun. **11**, 1904 (2009)
4. L. Hong, H. Xian-Deng, L. Zhou, Chin. J. Anal. Chem. **43**, 1291 (2015)
5. P. Makam, R. Shilpa, A.E. Kandjani, S.R. Periasamy, Y.M. Sabri, C. Madhu, S.K. Bhargava, T. Govindaraju, Biosens. Bioelectron. **100**, 556 (2018)
6. Y. Liu, X. Wang, H. Wu, Biosens. Bioelectron. **87**, 129 (2017)
7. H. Guo, J. Li, Y. Li, D. Wu, H. Ma, Q. Wei, B. Du, New J. Chem. **42**, 11147 (2018)
8. S.K. Kim, M. Gupta, H.-I. Lee, Sens. Actuators B Chem. **257**, 728 (2018)
9. V. Amani, R. Alizadeh, H.S. Alavije, S.F. Heydari, M. Abafat, J. Mol. Struct. **1142**, 92 (2017)
10. F. Domanico, G. Forte, C. Majorani, O. Senofonte, F. Petrucci, V. Pezzi, A. Alimonti, J. Trace Elem. Med. Biol. **43**, 3 (2017)
11. M.R.R. Kahkha, S. Daliran, A.R. Oveisi, M. Kaykhaii, Z. Sepehri, Food Anal. Methods **10**, 2175 (2017)
12. J.-L. Chen, P.-C. Yang, T. Wu, Y.-W. Lin, Spectrochim. Acta Part A Mol. Biomol. Spectrosc. **199**, 301 (2018)
13. Y. Yamini, M. Safari, Microchem. J. **143**, 503 (2018)
14. C. Gao, Q. Wang, F. Gao, F. Gao, Chem. Commun. **50**, 9397 (2014)
15. J. Tu, Y. Gan, T. Liang, Q. Hu, Q. Wang, T. Ren, Q. Sun, H. Wan, P. Wang, Front. Chem. **6**, 333 (2018)
16. X. Song, B. Fu, Y. Lan, Y. Chen, Y. Wei, C. Dong, Spectrochim. Acta Part A Mol. Biomol. Spectrosc. **204**, 301 (2018)
17. S.K. Daniel, A. Kumar, K. Sivasakthi, C.S. Thakur, Sens. Actuators B Chem. **290**, 73 (2019)
18. C. Rullyani, M. Shellaiah, M. Ramesh, H.-C. Lin, C.-W. Chu, Org. Electron. **69**, 275 (2019)
19. Q.-L. Wang, H.-F. Cui, X. Song, S.-F. Fan, L.-L. Chen, M.-M. Li, Z.-Y. Li, Sens. Actuators B Chem. **260**, 48 (2018)
20. Y. Zhang, J. Xia, F. Zhang, Z. Wang, Q. Liu, Sens. Actuators B Chem. **267**, 412 (2018)
21. S. Liu. Y. Wang. W. Xu. X. Leng. H. Wang. Y. Guo, J. Huang, Biosensors and Bioelectronics 88 (2017) 181
22. G. Shen, X. Zhang, S. Zhang, J. Electrochem. Soc. **161**, B256 (2014)
23. H.B. Seo, M.B. Gu, J. Biol. Eng. **11**, 11 (2017)
24. M.C. Rodriguez, A.-N. Kawde, J. Wang, Chem. Commun. **34**, 4267 (2005)
25. A. Abi, Z. Mohammadpour, X. Zuo, A. Safavi, Biosens. Bioelectron. **102**, 479 (2018)
26. D. Li, A. Wieckowska, I. Willner, Angew. Chem. Int. Ed. **47**, 3927 (2008)
27. C.H. Chung, J.H. Kim, J. Jung, B.H. Chung, Biosens. Bioelectron. **41**, 827 (2013)
28. E. Xiong, L. Wu, J. Zhou, P. Yu, X. Zhang, J. Chen, Anal. Chim. Acta **853**, 242 (2015)
29. C. Tortolini, P. Bollella, M.L. Antonelli, R. Antiochia, F. Mazzei, G. Favero, Biosens. Bioelectron. **67**, 524 (2015)
30. D. Han, Y.-R. Kim, J.-W. Oh, T.H. Kim, R.K. Mahajan, J.S. Kim, H. Kim, Analyst **134**, 1857 (2009)
31. B. Seiwert, U. Karst, Anal. Bioanal. Chem. **390**, 181 (2008)
32. A. Anne, A. Bouchardon, J. Moiroux, J. Am. Chem. Soc. **125**, 1112 (2003)
33. S. Yu, Y. Tang, Z. Li, K. Chen, X. Ding, B. Yu, Photonics Res. **6**, 90 (2018)
34. H. Huang, J.-J. Zhu, Analyst **138**, 5855 (2013)
35. O. Goryacheva, P. Mishra, Y.I. Goryacheva, Talanta **179**, 456 (2017)
36. M. Pedrero, S. Campuzano, J.M. Pingarrón, J. AOAC Int. **100**, 950 (2017)
37. R. Bala, A. Swami, I. Tabujew, K. Peneva, N. Wangoo, R.K. Sharma, Biosens. Bioelectron. **104**, 45 (2017)
38. Y.-P. Wei, X.-P. Liu, C.-J. Mao, H.-L. Niu, J.-M. Song, B.-K. Jin, Biosens. Bioelectron. **103**, 99 (2018)
39. A. Sun, J. Chai, T. Xiao, X. Shi, X. Li, Q. Zhao, D. Li, J. Chen, Sens. Actuators B Chem. **258**, 408 (2018)
40. H.N. Abdelhamid, H.-F. Wu, Spectrochim. Acta Part A Mol. Biomol. Spectrosc. **188**, 50 (2018)
41. H. Kim, J.D. Song, Appl. Surf. Sci. **427**, 405 (2018)
42. X. Cui, V.A. Lee, Y. Raphael, J.A. Wiler, J.F. Hetke, D.J. Anderson, D.C. Martin, J. Biomed. Mater. Res. Part A **56**, 261 (2001)
43. P.D. Tran, A. Le Goff, J. Heidkamp, B. Jousselme, N. Guillet, S. Palacin, H. Dau, M. Fontecave, V. Artero, Angew. Chem. **123**, 1407 (2011)
44. T. Kilic, A. Erdem, Y. Erac, M.O. Seydibeyoglu, S. Okur, M. Ozsoz, Electroanalysis **27**, 317 (2015)
45. P. Lee, K. Ward, K. Tschulik, G. Chapman, R. Compton, Electroanalysis **26**, 366 (2014)
46. S. Sharma, N. Singh, V. Tomar, R. Chandra, Biosens. Bioelectron. **107**, 76 (2018)
47. D.R. Kumar, S. Kesavan, M.L. Baynosa, J.-J. Shim, Electrochim. Acta **246**, 1131 (2017)
48. M. Safari, S. Najafi, E. Arkan, S. Amani, M. Shahlaei, Microchem. J. **146**, 293 (2019)
49. P. Dai, G. Zhang, Y. Chen, H. Jiang, Z. Feng, Z. Lin, J. Zhan, Chem. Commun. **48**, 3006 (2012)
50. Y. Liu, J. Lei, Y. Huang, H. Ju, Anal. Chem. **86**, 8735 (2014)
51. M. Shamsipur, A. Pashabadi, F. Molaabasi, S. Hosseinkhani, Biosens. Bioelectron. **90**, 195 (2017)
52. X. Li, X. Niu, W. Zhao, W. Chen, C. Yin, Y. Men, G. Li, W. Sun, Electrochem. Commun. **86**, 68 (2018)
53. W. Chen, W. Weng, C. Yin, X. Niu, G. Li, H. Xie, J. Liu, W. Sun, Int. J. Electrochem. Sci **13**, 4741 (2018)
54. S.A. Frank, F1000Research **7**, 200 (2018)
55. H. Ehzari, M. Safari, M. Shahlaei, Microchem. J. **143**, 118 (2018)
56. X. Zhu, L. Chen, Z. Lin, B. Qiu, G. Chen, Chem. Commun. **46**, 3149 (2010)
57. J. Wan, G. Yin, X. Ma, L. Xing, X. Luo, Electroanalysis **26**, 823 (2014)

58. H. Park, S.-J. Hwang, K. Kim, Electrochem. Commun. **24**, 100 (2012)
59. N. Zhou, J. Li, H. Chen, C. Liao, L. Chen, Analyst **138**, 1091 (2013)
60. J. Tang, Y. Huang, C. Zhang, H. Liu, D. Tang, Microchim. Acta **183**, 1805 (2016)
61. J. Chen, J. Tang, J. Zhou, L. Zhang, G. Chen, D. Tang, Anal. Chim. Acta **810**, 10 (2014)
62. Z. Lin, X. Li, H.-B. Kraatz, Anal. Chem. **83**, 6896 (2011)
63. S. Tang, P. Tong, W. Lu, J. Chen, Z. Yan, L. Zhang, Biosens. Bioelectron. **59**, 1 (2014)
64. J. Li, M. Sun, X. Wei, L. Zhang, Y. Zhang, Biosens. Bioelectron. **74**, 423 (2015)
65. J. Chen, S. Zhou, J. Wen, Anal. Chem. **86**, 3108 (2014)
66. S.-H. Wu, B. Zhang, F.-F. Wang, Z.-Z. Mi, J.-J. Sun, Biosens. Bioelectron. **104**, 145 (2018)
67. Y.L. Huang, Z.F. Gao, J. Jia, H.Q. Luo, N.B. Li, J. Hazard. Mater. **308**, 173 (2016)
68. R.-F. Huang, H.-X. Liu, Q.-Q. Gai, G.-J. Liu, Z. Wei, Biosens. Bioelectron. **71**, 194 (2015)
69. T. Bao, W. Wen, L. Shu, X. Zhang, S. Wang, New J. Chem. **40**, 6686 (2016)
70. S. Amiri, A. Navaee, A. Salimi, R. Ahmadi, Electrochem. Commun. **78**, 21 (2017)
71. M. Lu, R. Xiao, X. Zhang, J. Niu, X. Zhang, Y. Wang, Biosens. Bioelectron. **85**, 267 (2016)
72. B. Babamiri, A. Salimi, R. Hallaj, Biosens. Bioelectron. **102**, 328 (2018)